Modeling of Particle Transport on Channels and Gaps Exposed to Plasma Fluxes

Martin Nieto-Pérez
Instituto Tecnológico de Toluca
Av. Tecnológico S/N Col. La Virgen
Metepec, Mexico, 52140 MEXICO

Abstract. Many problems in particle transport in fusion devices involve the transport of plasma or eroded particles through channels or gaps, such as in the case of trying to assess damage to delicate optical diagnostics collecting light through a slit or determining the deposition and codeposition on the gaps between tiles of plasma-facing components. A dynamic-composition Monte Carlo code in the spirit of TRIDYN, previously developed to study composition changes on optical mirrors subject to ion bombardment, has been upgraded to include motion of particles through a volume defined by sets of plane surfaces. Particles sputtered or reflected from the walls of the channel/gap can be tracked as well, allowing the calculation of wall impurity transport, either back to the plasma (for the case of a gap) or to components separated from the plasma by a channel/slit (for the case of optical diagnostics). Two examples of the code application to particle transport in fusion devices will be presented in this work: one will evaluate the erosion/impurity deposition rate on a mirror separated from a plasma source by a slit; the other case will look at the enhanced emission of tile material in the region of the gap between two tiles.

Keywords: Plasma-facing components, diagnostics, irradiation damage, sputtering, Monte Carlo simulations.
PACS: 52.40.Hf, 52.65.Pp, 61.80.Jh

INTRODUCTION

The understanding of plasma-material interactions in fusion reactors is crucial in the development of a commercial fusion reactor. The study of such interactions is a vast and active field, with an excellent literature review available elsewhere[1]. In particular, the issue of impurity transport and control has received significant attention since impurities play important roles in reactor performance depending on where they are: core impurities cool the plasma by increasing Z_{eff}, while edge impurities are very effective at shielding plasma-facing components (PFCs) against heat in detached operation[2]. Impurity transport is also responsible for the formation of mixed surfaces, such as the case of first wall material depositing on divertor plates. Such mixed materials have different properties than the original materials, a fact that may have significant impact on the interaction between the component and the plasma[3].

Since most PFCs are generally surfaces composed of several tiles, there are a number of gaps in the plasma-facing surface. The role of such gaps was recognized as critical when it was found that about 30% of the tritium retained in the TEXTOR tiles was located in the gaps between them[4]. This has triggered an experimental[5, 6] and computational[7, 8] effort to look in more detail at the transport of particles in this type of

regions. In the present paper, a previously developed Monte Carlo code[9] in the spirit of the TRIDYN code[10], with the added capability of geometric particle tracking, is used to study particle transport in a gap due to physical sputtering of gap material, varying the gap depth/width ratio and the main angle of incidence of the plasma. Because of the similarity, the study is extended to analyze another critical issue in impurity transport[11]: the effect on plasma exposure on an optical diagnostic exposed to the plasma by means of a slit.

DESCRIPTION OF THE SIMULATIONS

The first case analyzed was a gap between two graphite tiles, with a geometry shown in Figure 1a. The gap has depth d in the z-direction and width w in the x-direction. Since the gap length in the y- direction is assumed to be large compared to w, periodic boundaries at $y = 0$ and $y = w$ were used in the simulation. The plasma is a plane at $z = 0$, emitting D-T particles with equal probability with a Maxwell distribution having $T_i = 40$ eV and a Lambertian (cosine) angular distribution. Counting planes are placed in front of each solid surface and at the exit of the gap for measuring gap wall and bottom erosion, as well as gap material emission to the plasma. The parameter varied during the simulation was the gap depth d, normalized to w. The effect of the main angle of incidence was considered by running another simulation with the plasma plane tilted 45° with respect to the gap entrance.

The other case discussed in the present work is a slit separating a plasma and a mirror, with the geometry shown in Figure 1b. The slit has depth d in the z-direction and width w in both the x- and y-direction (square slit). The walls of the slit are assumed to be iron, since a steel shield would be mostly iron, while the mirror is assumed to be made out of molybdenum, with a tilt of 45° in the y-axis with respect to the slit exit plane. The plasma is again at $z = 0$ with the same conditions as in the previous case, except that this time a 1% beryllium impurity with the same energy and angle distribution is introduced in order to evaluate its effect on the mirror. The simulation of particle transport in this system is done for a short (d/w=1) and a long (d/w=10) slit, and the mirror surface is treated as a dynamic target where implantation and erosion can modify the surface composition.

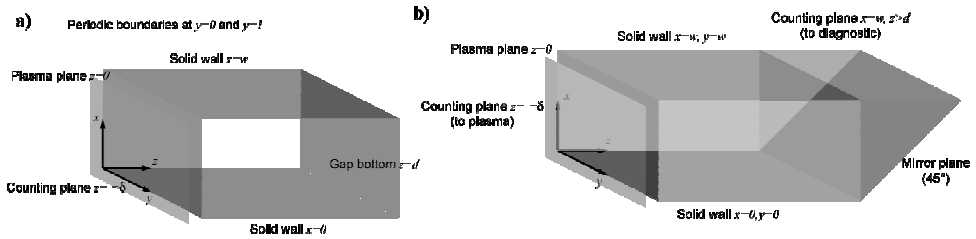

FIGURE 1. Geometries used in the simulation of a) a gap between two tiles, and b) the slit of an optical diagnostic

RESULTS AND DISCUSSION

One of the most important questions regarding gaps between tiles is: what is the critical depth beyond which the erosion does not change anymore? To answer that question, Figure 1 plots the carbon yield as a function of d/w, showing how the sputtering yield increases as the gap depth increases. However, for values of $d/w > 5$ the curve seems to level off, both for the plasma plane parallel to the opening and the one tilted 45°. The erosion of the bottom surface of the gap is also reduced as the gap depth increases, and it does so in an exponential fashion as evidenced in Figure 2. For shallow gaps, most of the material ejected from the gap comes from the bottom, the limit being $d = 0$ where all the material sputtered comes from the "bottom". This is especially important if the material on the gap bottom is easily sputtered, or if its erosion may result in component failure, such as a cooling component. The decay constant of the bottom surface sputtering yield is expected to be a function of the gap material: materials easily sputtered (i.e. Be, C) will have larger decay constants, while materials with low sputtering yields (i.e. W) will have shorter decay constants. That type of study is left as the subject for a future paper.

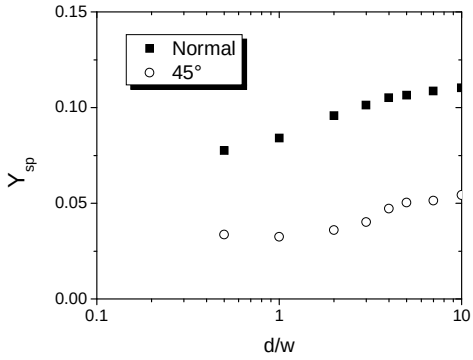

FIGURE 1. Total sputtering yield of gap material as a function of gap depth, for a plasma plane parallel to the opening and tilted 45°.

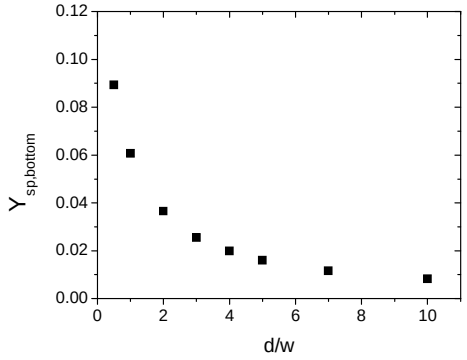

FIGURE 2. Total sputtering yield of gap material as a function of gap depth, for a plasma plane parallel to the opening and tilted 45°.

For the case of the optical diagnostics, two important mechanisms may degrade the performance of an optical diagnostic exposed to plasmas: physical erosion leading to roughening and material depletion, and deposition of impurities in the surface that

may modify the optical properties. In the simulation presented here, three types of impurities are considered: a Be intrinsic plasma impurity (1% of DT flux), Fe impurities due to the slit bombardment, and Mo impurities from the first mirror erosion. The simulation is run to a fluence value of $2x10^{19}$ cm^{-2}, equivalent to a 1 ms pulse with ~ $2x10^{22}$ cm^{-2} s^{-1}, comparable to ITER edge conditions[12].

The relative fractions of these three impurities in the impurity flux into the diagnostic (plane $x = w$, $z > d$ in Figure 1b) are shown in Figure 3 (the balance of this flux is DT particles) as a function of plasma fluence. The main impurity reaching the exit plane is Fe, followed by Mo and Be. The concentrations of Be and Fe are also tracked on the mirror surface, but the erosion of the mirror is too fast to allow for any impurity buildup and the surface remains unchanged throughout the simulation. The mirror is eroded 20 nm with a fluence of 2 x 10^{19} cm^{-2} when $d/w = 1$, as seen in Figure 4, so the mirror would erode that amount per 1 ms ITER shot. This means that the problem of mirror outweighs mirror contamination for the case of the first mirror. If the slit is 10 times longer (d/w=10), the mirror sputtering is greatly suppressed and the thickness stays fairly constant, with the surface still being essentially free of contaminants. For this case, the flux reaching the diagnostic interior is two orders of magnitude and Mo is the main impurity, followed by Fe.

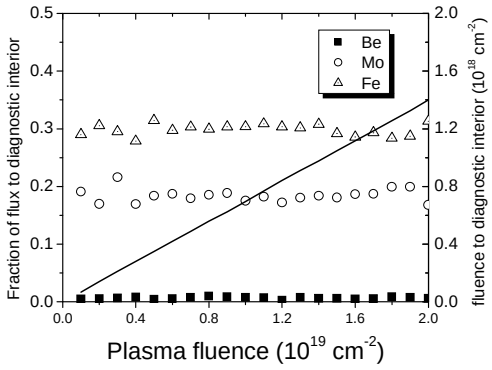

FIGURE 3. Fluence entering the diagnostic beyond the first mirror (solid line, right axis) and its composition (symbols, left axis). The remainder of the composition is DT

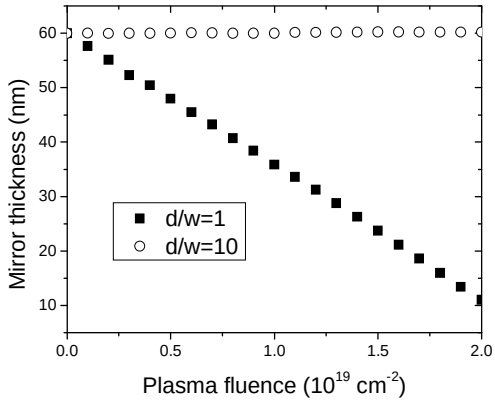

FIGURE 4. Erosion of the first mirror vs. fluence for a short (d/w=1) and a long (d/w=10) slit.

CONCLUSIONS

The transport of material due to physical sputtering on both a PFC tile gap and an optical diagnostic slit has been studied using a dynamic Monte Carlo code. For the case of the gap, it was found that the amount of sputtered material increases with depth up to a certain point, beyond which the amount of sputtered material levels off. Comparing erosion due to a plasma plane parallel to the gap opening with one tilted 45°, it was found that the parallel plane is more effective at removing material from the gap, eroding twice as fast compared to the 45° plane. For the case of the slit, it was found that for the case of a short slit with equal depth and width the mirror erosion is the main problem, since about 10 nm of mirror material are eroded when exposed to a 10^{22} cm^{-2} s^{-1} flux for 1 ms. Three types of impurities that may reach the diagnostic interior were considered: intrinsic plasma impurities (Be), slit material (Fe) and eroded first mirror material (Mo). The three are able to reach the diagnostic interior, along with D-T particles from the plasma. The dynamic simulation of the mirror surface showed no evidence of surface contamination, since the sputtering is much faster than the rate of impurity implantation. Extension of the slit depth reduces the flux of particles beyond the first mirror by 2 orders of magnitude. For this case, almost no erosion of the first mirror occurs, the main impurity entering the diagnostic is Mo, and no Be goes beyond the first mirror. The surface starts to build up impurities (mostly Fe), but simulations at much larger fluences may be necessary to quantify their effect.

ACKNOWLEDGMENTS

The author wishes to acknowledge the International Atomic Energy Agency for providing funding that allowed the author to present this work.

REFERENCES

1. R. Parker, G. Janeschitz, H.D. Pacher et al. *J. Nuc. Mat.* **241 – 243**, p. 1 (1997).
2. K. Shimizu, T. Takizuka, A. Sakasai. *J. Nuc. Mat.* **241 – 243**, p. 167 (1997).
3. R. P. Doerner.. *J. Nuc. Mat.* **363 - 365**, p. 32 (2007).
4. A. Litnovsky, V. Phillips, P. Wienhold et al. *J. Nuc. Mat.* **337-339**, p. 917 (2005).
5. C.P.C. Wong, D.L. Rudakov, J.P. Allain et al. *J. Nuc. Mat.* **363 - 365**, p. 276 (2007)
6. K. Krieger, W. Jacob, D.L. Rudakov et al. *J. Nuc. Mat.* **363 - 365**, p. 870 (2007).
7. G. Federici, M. Mayer, G. Strohmayer et al. *J. Nuc. Mat.* **337-339**, p. 40 (2005).
8. R. Dejarnac, J.P. Gunn. *J. Nuc. Mat.* **363 - 365**, p. 560 (2007).
9. J. P. Allain, M. Nieto, A. Hassanein et al. *Proc. SPIE* **6151** n. II p. 615131 (2006).
10. W. Möller, W. Eckstein, J. P. Biersack. *Comp. Phys. Comm.* **51** (1988) 355.
11 G. De Temmerman, R.A. Pitts, V.S. Voitsenya et al.. *J. Nuc. Mat.* **363 - 365**, p. 259 (2007)..
12. A. Loarte, B. Lipschultz, A.S. Kukushkin et al. *Nuclear Fusion* **47**, p. S203 (2007).